

Altered whole-brain resting-state functional connectivity and brain network topology in typhoon-related post-traumatic stress disorder

Hui Juan Chen*, Jun Ke*, Jie Qiu, Qiang Xu, Yuan Zhong, Guang Ming Lu, Yanglei Wu, Rongfeng Qi and Feng Chen 

Ther Adv Psychopharmacol

2023, Vol. 13: 1–14

DOI: 10.1177/
20451253231175302

© The Author(s), 2023.
Article reuse guidelines:
[sagepub.com/journals-](https://sagepub.com/journals-permissions)
permissions

Abstract

Background: Altered resting-state functional connectivity has been found in patients with post-traumatic stress disorder (PTSD). However, the alteration of resting-state functional connectivity at whole-brain level in typhoon-traumatized individuals with PTSD remains largely unknown.

Objectives: To investigate changes in whole-brain resting-state functional connectivity and brain network topology in typhoon-traumatized subjects with and without PTSD.

Design: Cross-sectional study.

Methods: Twenty-seven patients with typhoon-related PTSD, 33 trauma-exposed controls (TEC), and 30 healthy controls (HC) underwent resting-state functional MRI scanning. The whole brain resting-state functional connectivity network was constructed based on the automated anatomical labeling atlas. The graph theory method was used to analyze the topological properties of the large-scale resting-state functional connectivity network. Whole-brain resting-state functional connectivity and the topological network property were compared by analyzing the variance.

Results: There was no significant difference in the area under the curve of γ , λ , σ , global efficiency, and local efficiency among the three groups. The PTSD group showed increased dorsal cingulate cortex (dACC) resting-state functional connectivity with the postcentral gyrus (PoCG) and paracentral lobe and increased nodal betweenness centrality in the precuneus relative to both control groups. Compared with the PTSD and HC groups, the TEC group showed increased resting-state functional connectivity between the hippocampus and PoCG and increased connectivity strength in the putamen. In addition, compared with the HC group, both the PTSD and TEC groups showed increased connectivity strength and nodal efficiency in the insula.

Conclusion: Aberrant resting-state functional connectivity and topology were found in all trauma-exposed individuals. These findings broaden our knowledge of the neuropathological mechanisms of PTSD.

Keywords: functional connectome, functional magnetic resonance imaging, graph theory, post-traumatic stress disorder, small worldness

Received: 26 September 2022; revised manuscript accepted: 24 April 2023.

Introduction

Post-traumatic stress disorder (PTSD) is a psychiatric disorder that occurs in some individuals after

they experience, witness, or hear about events involving death or serious physical injuries (which have occurred or not), such as military wars,

Correspondence to:

Rongfeng Qi

Department of Medical Imaging, Jinling Hospital, Medical School, Nanjing University, Nanjing 210002, Jiangsu, China.

fmriqirf@126.com

Feng Chen

Department of Radiology, Hainan General Hospital (Hainan Affiliated Hospital of Hainan Medical University), No. 19, Xiuhua Street, Xiuying District, Haikou 570311, Hainan, China.

fenger0802@163.com

Hui Juan Chen

Department of Radiology, Hainan General Hospital (Hainan Affiliated Hospital of Hainan Medical University), Haikou, China

Jun Ke

Department of Medical Imaging, Jinling Hospital, Medical School, Nanjing University, Nanjing, China

Department of Radiology, The First Affiliated Hospital of Soochow University, Suzhou, China

Jie Qiu

Department of Ultrasound, Hainan General Hospital (Hainan Affiliated Hospital of Hainan Medical University), Haikou, China

Qiang Xu

Yuan Zhong

Guang Ming Lu

Department of Medical Imaging, Jinling Hospital, Medical School, Nanjing University, Nanjing, China

Yanglei Wu

MR Collaboration, Siemens Healthineers Ltd., Beijing, China

*These authors contributed equally to this work.

traffic accidents, or natural disasters.¹ Clinically, PTSD is characterized by perceived repeated traumatic experiences, negative emotions, and cognitive effects, avoidance of any scene that causes a traumatic memory, and high alertness.¹ In addition, PTSD is often associated with mental diseases (e.g. major depression), risk of substance abuse, and physiologic diseases (e.g. cardiovascular disease, diabetes).^{2,3} Although medication and psychotherapy have played a major role in PTSD treatment, some patients are resistant to existing treatment methods or the methods may have poor efficacy.⁴ Therefore, it is necessary to further study the neuropathogenesis of PTSD and develop more targeted interventions.

Functional connectivity that assesses the intensity of the connectivity between brain regions has advanced our knowledge regarding PTSD neuropathogenesis. Recently, a ‘three-network’ model has been proposed. The model suggested that many neuropsychiatric diseases, including PTSD, have local brain function or resting-state functional connectivity abnormalities in the default mode network (DMN), salience network (SN), and executive control network (ECN).⁵ The DMN, including the medial prefrontal cortex, posterior cingulate/precuneus, and lateral parietal cortex, is associated with autobiographical memory and self-reference processing.⁶ The SN mainly comprises the amygdala, insula, and dorsal portion of the anterior cingulate cortex and plays a vital role in attention processing.⁷ The ECN primarily comprises the dorsolateral prefrontal cortex and lateral parietal cortex, which play an important role in memory and attention control.⁸ However, some studies have revealed that the resting-state functional connectivity of some brain regions outside the resting-state network in PTSD patients has also changed,^{9–11} suggesting that the whole-brain resting-state functional connectivity network may be abnormal. Few studies have investigated whole-brain resting-state functional connectivity in PTSD patients. Jin *et al.* found that the positive resting-state functional connectivity between the orbitofrontal gyrus and hippocampus, middle frontal gyrus and amygdala, and hippocampus and rectus gyrus in PTSD patients was reduced compared with trauma-exposed controls among earthquake survivors.¹² Negative resting-state functional connectivity was enhanced between the posterior cingulate cortex and insular cortex.¹² However, the study did not include people who had not experienced trauma as controls, so it

was impossible to determine whether resting-state functional connectivity abnormalities were PTSD-specific or trauma-related.

The graph-based network method focuses on the regional and network-level topological characteristics of the brain.¹³ Functional magnetic resonance imaging (fMRI)¹⁴ research has revealed that non-traumatized people have significant small-world properties in large-scale functional brain networks. Specifically, the clustering coefficient is higher than that of random networks and the characteristic shortest path length is lower than in regular networks. The small-world property of the human brain network reflects its features of functional separation and functional integration,¹⁵ which enable different brain regions to exchange information efficiently. Research has shown that the small-world nature of the human brain network is disrupted in depression^{16,17} and schizophrenia.¹⁸ Though abnormal small-world properties have been reported in PTSD patients,^{19–21} results are inconsistent and limited.

In addition to changes in the global parameters of brain networks, other reports have also revealed that PTSD patients showed altered local parameters of multiple brain regions, including in the DMN, SN, or ECN.^{19–21} The differences in the results of brain networks in the above studies may be associated with differences in imaging modalities and control groups. In addition, these studies did not include the trauma control and healthy control groups, so it is unclear whether trauma can cause changes in the brain network’s topological properties. It should be noted that PTSD caused by different trauma types may have different brain function damage patterns.²² Therefore, the effects of other types of trauma-induced PTSD on the topological properties of individual large-scale brain networks need to be studied further.

In this study, we compared the whole-brain resting-state functional connectivity of typhoon-related PTSD patients, trauma-exposed controls (who had the same trauma experience but did not develop PTSD, TEC), and healthy controls (who did not experience typhoon trauma, HC). We hypothesized that PTSD patients and trauma-exposed controls have abnormal resting-state functional connectivity in multiple brain regions, including the DMN and SN. In addition, the topological properties were explored based on the graph theory, and we assumed that the global and

local parameters of the whole-brain network would change in PTSD patients and traumatized controls. Finally, we investigated the relationship between brain function changes and clinical symptoms by correlating resting-state functional connectivity and global and local parameters of the brain network with the Clinical Administred PTSD Scale (CAPS) and PTSD checklist (PCL) scores of patients.

Materials and methods

Participants

The ninth super typhoon ‘Rammasun’ in 2014 was the strongest typhoon to land on the coast of South China over the past 40 years. On 18 July 2014, the typhoon hit the coast of Wenchang City, Hainan Province, causing substantial economic losses and psychological trauma to the residents.

For this study, we recruited from Wenchang City 36 patients with typhoon-related PTSD (9 men and 27 women), 34 typhoon-related TEC (7 men and 27 women), and 32 not traumatized subjects (healthy controls, HC) from Haikou City who did not experience the typhoon (9 men and 23 women). All the typhoon-experienced patients were screened using PCL,²³ and those with a score greater than 35 were assessed using the Diagnostic and Statistical Manual of Mental Disorders, Fourth Edition, Axis I Clinical Structured Interview^{24,25} to verify whether they met the diagnostic criteria for PTSD and other mental disorders. The symptoms of PTSD patients were further assessed using the CAPS scale.²⁶ The Self-Rating Anxiety Scale (SAS)²⁷ and Self-Rating Depression Scale (SDS)²⁸ were used to evaluate anxiety and depressive symptoms in all subjects. The clinical screening and evaluation work was completed by psychiatrists at the Second Xiangya Hospital of Central South University from 2014 to 2015.

Subjects were excluded if they met one of the following criteria: age less than 18 or more than 65 years, any history of major physical illness, psychiatric disorders, head injury, recent alcohol or drug intake, pregnancy, left-handedness, contraindications to MRI, and excessive head movement (translation > 1.5 mm or rotation > 1.5°)²⁹ during the MRI. Nine patients with PTSD (three women had no useful image data), two with metal denture artifacts (one man and one woman), one woman with cerebral infarction, one pregnant

woman, and two patients with excessive head movement (one man and one woman) were excluded. In addition, one female TEC and two male HCs were excluded due to excessive head movement and cerebral infarction, respectively. Therefore, 27 PTSD patients, 33 TEC, and 30 HCs were enrolled in the present study. All subjects were informed of the details of the study, and informed consent was obtained. Approval for this study was waived by the ethics committee of our hospital and the Second Xiangya Hospital (Number 20140306).

MRI data acquisition

MRI images were acquired on a Siemens Skyra 3T superconducting MR imager with a standard head coil, and the scanning was completed in the Department of Radiology, Hainan General Hospital. During the MRI scan, each subject was instructed to lie on his or her back, close his or her eyes, relax, and stay awake. The head was fixed with a sponge cushion. Resting-state functional images were acquired with a GRE-EPI (gradient-echo-planar echo-planar-imaging) sequence, with the imaging plane parallel to the anterior and posterior commissure. The parameters were as follows: repetition time (TR) = 2000 ms, echo time (TE) = 30 ms, flip angle = 90°, field of view = 230 × 230 mm², matrix = 64 × 64, slices = 35, slice thickness = 3.6 mm, no slice spacing, and 250 time points. High-resolution T1-weighted three-dimensional structural images were acquired using the sagittal magnetization-prepared rapid gradient echo sequence. The detailed parameters were as follows: TR = 2300 ms, TE = 1.97 ms, flip angle = 9°, field of view = 256 × 256 mm², matrix = 256 × 256, slices = 176, and slice thickness = 1 mm.

Data preprocessing

The SPM8 (<http://www.fil.ion.ucl.ac.uk/spm/>) toolbox based on the Matrix laboratory (MATLAB) software was used to preprocess the fMRI data. The first 10 volumes of the images were discarded to ensure the stability of the obtained signal. The remaining 240 volumes were used to correct time and head motion. The functional images were then spatially normalized to the Montreal Neurological Institute (MNI) standard space, with a resampling size of 3 × 3 × 3 mm³. The fMRI data were then processed using Resting-State fMRI Data Analysis Toolkit 1.8 (<http://www.restfmri.net>) software to

remove the linear drift and band-pass filtering (0.01–0.08 Hz), followed by regression analysis of the covariates, including the mean signals of the whole brain, white matter, and cerebrospinal fluid, and six parameters obtained during the head movement correction process. Finally, the fMRI data were smoothed with a Gaussian kernel of 8 mm with a full width at half-maximum.

Network construction and analysis

The functional connection network was constructed using GRETNA software (www.nitrc.org/projects/Gretna/). Specifically, we used the automated anatomical labeling (AAL) template to divide the brain into 90 cortical and subcortical regions. Then, the mean time series of each brain region was extracted, and Pearson correlation analysis was performed to obtain a 90×90 correlation coefficient matrix. In addition, the correlation coefficient was transformed by Fisher Z to obtain the whole brain resting-state functional connectivity network.

Each of the above brain regions was defined as a node of the network to create a weighted brain resting-state functional connectivity network, and the weight of each ‘edge’ was delineated as the absolute strength of resting-state functional connectivity between the connected regions. Finally, we analyzed the topological properties of the weighted brain resting-state functional connectivity network based on graph theory. Because the number of ‘edges’ affected the analysis results of the topological properties of the brain network, we matched the number of ‘edges’ of the weighted brain resting-state functional connectivity network of each subject by setting the sparsity (S). S is the fraction of the maximum possible number of ‘edges’ that remain after setting the threshold for the strength of the functional connection.

In this study, the threshold range of S was determined based on the following standards: the average nodal degree of the brain network corresponding to the minimum value of S was greater than $2 \ln(N)$, where N refers to the node number; and the small-world attribute of the brain network corresponding to the maximum value of S was greater than 1.1. Researchers believe that S can ensure the assessment of the small-world property of the network under different levels of sparsity and minimize the number of false ‘edges’. According to this criterion, the S range of the midbrain network in this study was set at 0.1 to 0.36, with an interval of 0.01.

We calculated seven standard global parameters of brain networks: the weighted clustering coefficient (Cnet), weighted characteristic shortest path length (Lnet), normalized weighted clustering coefficient (γ), normalized weighted characteristic shortest path length (λ), small-worldness (σ), global efficiency (Eglob), and local efficiency (Eloc). Cnet reflected the local interconnectivity or cliquishness between nodes, and Lnet quantified the information transmission ability of the network. In addition, γ , λ , and σ were the ratios of Cnet to Crand, Lnet to Lrand, and γ to λ , respectively. Crand and Lrand were the weighted clustering coefficient and the weighted characteristic shortest path length of the random network, respectively. Generally speaking, the Cnet of small-world networks was significantly higher than Crand, whereas Lnet was similar to Lrand, so $\gamma > 1$, $\lambda \approx 1$, and $\sigma > 1$. Eglob evaluated the speed of information spreading in the brain network, and Eloc reflected the information exchangeability of the sub-network. In addition, three local parameters, weighted connectivity strength (Si), nodal efficiency (Ei), and nodal betweenness centrality (BCi), were calculated. Si was the sum of the absolute values (weights) of the functional connection strengths of all the edges of node I. Ei reflected the information transfer efficiency between node I and other nodes in the sub-network. Finally, BCi measured how much information within the subnetwork would pass through node I.

Statistical analysis

SPSS 16.0 software (IBM, USA) was used to compare the gender distribution of the three groups with the chi-square test. A two-sample *t*-test was applied to compare the PCL score of the PTSD and TEC groups. One-way analysis of variance (ANOVA) was used for age, years of education, SAS score, and SDS score comparison among the three groups. The threshold for statistical significance was set at $p < 0.05$.

The whole-brain resting-state functional connectivity of the three groups of subjects, with years of education and diagnosis of depression as covariates, was analyzed. We also included education, SAS and SDS scores as covariates for supplementary analysis. The group comparison results of whole-brain resting-state functional connectivity were corrected by the ‘false positive correction’ method,^{30,31} that is, $p < 1/4005 = 0.0002497$. This indicated that we expected less than one false-positive per analysis.³²

Table 1. Demographic and clinical data of traumatized individuals and healthy controls.

	PTSD (<i>n</i> =27)	TEC (<i>n</i> =33)	HC (<i>n</i> =30)	<i>p</i> -value
Sex (men/women)	7/20	7/26	7/23	0.912 ^a
Age (years)	48.4 ± 10.3	48.5 ± 7.5	49.9 ± 6.1	0.729 ^b
Education (years)	6.4 ± 3.4	7.0 ± 3.4	9.7 ± 3.3	<0.001 ^b
SAS score	65.8 ± 13.3	41.3 ± 8.1	36.0 ± 5.5	<0.001 ^b
SDS score	69.6 ± 13.2	41.3 ± 9.1	33.5 ± 7.2	<0.001 ^b
PCL score	53.7 ± 8.5	28.9 ± 5.4		<0.001 ^c
CAPS total score	78.2 ± 19.3			

CAPS, Clinician-Administered PTSD Scale; HC, healthy control; PCL, PTSD Checklist; PTSD, post-traumatic stress disorder; SAS, Self-Rating Anxiety Scale; SDS, Self-Rating Depression Scale; TEC, trauma-exposed control. Values are presented as mean ± SD except for sex, which is a number.

^a*p*-value obtained with chi-square test.

^b*p*-value obtained with one-way analysis of variance.

^c*p*-value obtained with independent *t*-test for continuous variables. Values are presented as mean ± SD except for sex, which is a number.

Because the method of ‘false positive correction’ is stricter for the multiple corrections of the results of the whole-brain resting-state functional connectivity analysis, we also set $p < 0.001$ (not corrected) as a relatively loose threshold to show the difference between the groups.

For γ , λ , and σ , we calculated the parameter values corresponding to each sparsity value. In addition, we calculated the area under the curve of seven global parameters and four local parameters with *S* and used the SPSS 16.0 software to analyze the area under the curve, with education and diagnosis of depression as covariates. The values of education, SAS and SDS scores were also included as covariates in the supplementary analysis. For the analysis of global parameters, the significance threshold level was set at $p < 0.05$. In addition, the ‘false-positive correction’ method was selected for multiple corrections of local parameters, that is, $p < 1/90 = 0.0111$.

The area under the comparison curve was chosen because this method can make an overall evaluation of the topological features of the brain network independent of sparsity. Then, we extracted the topological parameters of the brain regions and the strength of the resting-state functional connectivity of the brain regions (*Z*-value) with differences between the groups. Finally, the total CAPS score of the patients was correlated with the topological properties with the Pearson

correlation analysis. The correlation analysis was also conducted for the functional index and PCL score in all traumatized subjects.

Results

Demographic and clinical data

Table 1 demonstrates the general information and clinical parameters of the subjects. The differences in age and sex did not reach statistical significance among the three groups. The years of education in the HC group were higher than in the PTSD and TEC groups, but there was no significant difference between the PTSD and TEC groups. The PTSD group showed higher PCL scores than the TEC group. Of the 27 PTSD patients, 9 (2 men and 7 women) were diagnosed with depression, and 1 woman was diagnosed with anxiety. The TEC group scored less in SAS and SDS than the PTSD group but more than the HC group. The average score of CAPS in the PTSD group was 78.2.

Whole-brain resting-state functional connectivity

There were significant differences in resting-state functional connectivity between the right dorsal anterior cingulate cortex (dACC) and right paracentral lobule ($p = 0.000097$), right hippocampus and left postcentral gyrus (PoCG) ($p = 0.000385$),

Table 2. Global parameters of brain resting-state functional connectivity networks in traumatized individuals and healthy controls.

	PTSD	TEC	HC	p-value
C_{net}	0.05 ± 0.01	0.05 ± 0.01	0.05 ± 0.01	0.69 ^a
L_{net}	0.77 ± 0.04	0.76 ± 0.04	0.78 ± 0.05	0.54 ^a
Γ	0.44 ± 0.06	0.46 ± 0.06	0.48 ± 0.08	0.18 ^a
λ	0.32 ± 0.01	0.31 ± 0.01	0.32 ± 0.01	0.82 ^a
σ	0.36 ± 0.05	0.38 ± 0.05	0.40 ± 0.07	0.18 ^a
E_{glob}	0.09 ± 0.01	0.09 ± 0.01	0.09 ± 0.01	0.58 ^a
E_{loc}	0.13 ± 0.01	0.13 ± 0.01	0.12 ± 0.01	0.56 ^a

C_{net} , the weighted clustering coefficient; L_{net} , weighted characteristic shortest path length; γ , normalized weighted clustering coefficient; λ , normalized weighted characteristic shortest path length; σ , small worldness properties; E_{glob} , global efficiency; E_{loc} , local efficiency; HC, healthy control; PTSD, post-traumatic stress disorder; TEC, trauma-exposed control.

Covariates include education and diagnosis of depression.

^aThe results of covariance analysis.

right hippocampus and right PoCG ($p=0.000363$), and the left dorsal anterior cingulate gyrus and left PoCG ($p=0.000620$). The PTSD group showed higher positive resting-state functional connectivity between the right dorsal anterior cingulate gyrus and the right paracentral lobule compared with the TECs and HCs. These two brain regions mainly showed negative resting-state functional connectivity in the TEC and HC groups (Figures 1 and 2(a)). The negative resting-state functional connectivity of the right hippocampus to the left PoCG and the right PoCG was significantly lower in the TEC compared with the PTSD and HC groups (Figures 1 and 2(b) and (c)). The PTSD group also showed enhanced positive resting-state functional connectivity between the left dorsal anterior cingulate gyrus and the left PoCG relative to the TEC and HC groups (Figures 1 and 2(d)).

Global topology of brain resting-state functional connectivity network

As shown in Figure 3, when S was in the 0.1–0.36 range, the λ (Figure 3(a)) of the brain resting-state functional connectivity network of the PTSD, TEC, and HC groups was close to 1, whereas γ (Figure 3(a)) and σ (Figure 3(b)) were significantly greater than 1, suggesting that the brain networks of the three groups of subjects had typical small-world attributes. γ and σ showed a

decreasing trend from the HC group to the TEC group and to the PTSD group. However, there was no significant difference in the area under the curve of γ , λ , and σ among the three groups after the regression of covariates (Table 2). In addition, the area under the curve of E_{glob} and E_{loc} was not significantly different among the three groups (Table 2).

Local parameters of brain function connection network

There were significant differences in the area under the curve of S_i in the left insula ($p=0.003$), S_i in the right putamen ($p=0.011$), E_i in the left insula ($p=0.003$), and BC_i in the right precuneus ($p=0.009$). S_i in the left insula was higher in both the PTSD and TEC groups compared with the HC group (Figure 4(a)). The TEC group exhibited increased S_i in the right putamen relative to the PTSD and HC groups (Figure 4(b)). The PTSD and TEC groups had increased E_i in the left insula compared with the HC group (Figure 4(c)). The PTSD group had a higher BC_i in the right precuneus relative to both the TEC and HC groups (Figure 4(d)).

Resting-state functional connectivity and topology results including education, SAS and SDS scores as covariates were provided in the Supplementary material.

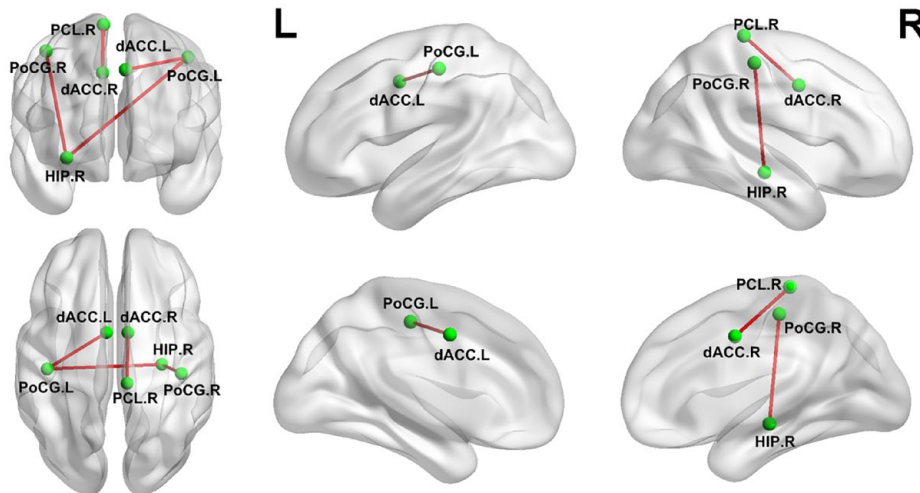


Figure 1. Brain regions with group differences in global resting-state functional connectivity. There were significant group differences in resting-state functional connectivity between the right dACC and right paracentral lobule, right hippocampus and left PoCG, right hippocampus and right PoCG, and the left dACC and left PoCG ($p < 0.001$). dACC, dorsal anterior cingulate; HIP, hippocampus; L, left; PCL, paracentral lobule; PoCG, postcentral gyrus; R, right.

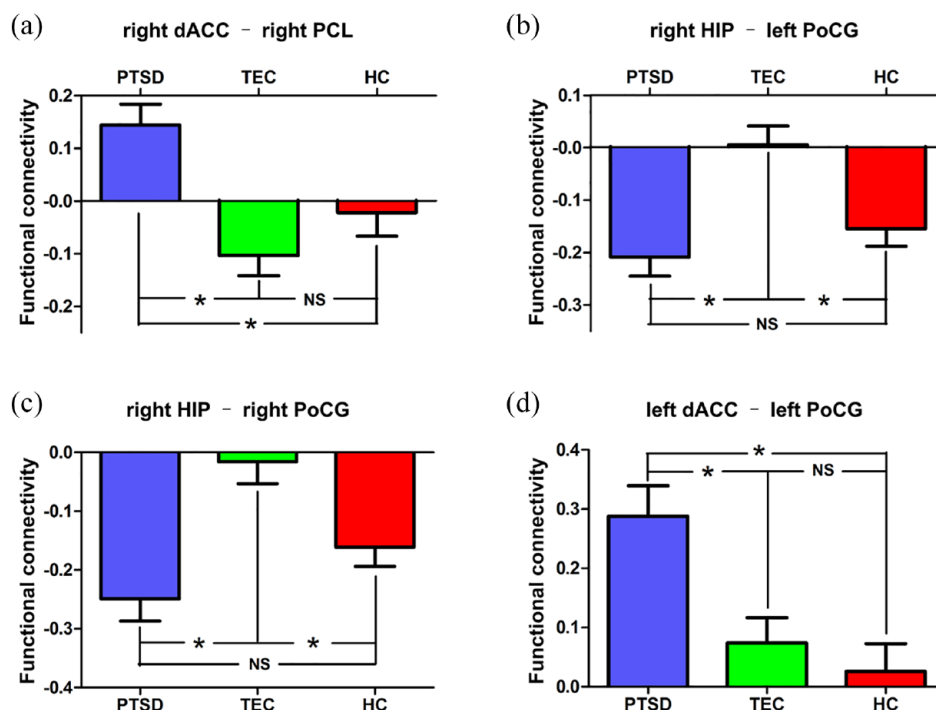


Figure 2. Results of post hoc t -tests of whole-brain resting-state functional connectivity. (a) The positive resting-state functional connectivity between the right dACC and right paracentral lobule was stronger in PTSD than in the TECs and HCs; (b) The negative resting-state functional connectivity between the right hippocampus and the left PoCG was weaker in the TECs than in the PTSD patients and HCs; (c) The negative resting-state functional connectivity between the right hippocampus and right PoCG in the TEC group was weaker than in the PTSD and HC groups; (d) The positive resting-state functional connectivity between the left dorsal anterior cingulate gyrus and left PoCG in the PTSD group was stronger than in the TEC and HC groups. dACC, dorsal anterior cingulate gyrus; HC, healthy control; HIP, hippocampus; PCL, paracentral lobule; PoCG, postcentral gyrus; PTSD, post-traumatic stress disorder; TEC, trauma-exposed control.

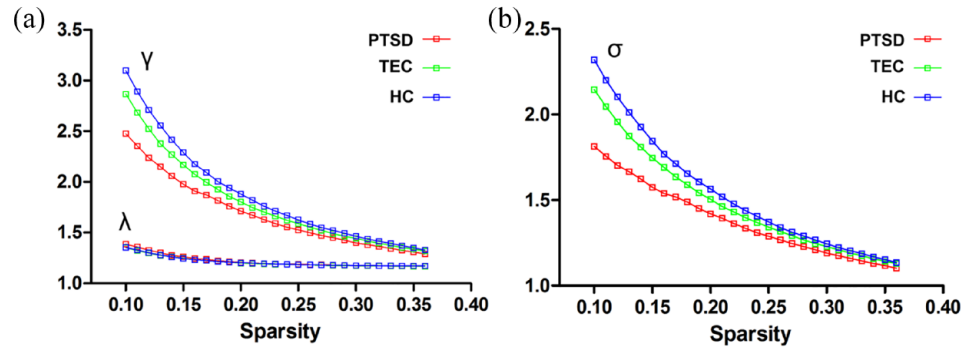


Figure 3. The γ , λ , and σ curves of the brain resting-state functional connectivity network with sparsity. (a) In the range of sparsity from 0.1 to 0.36, both γ and λ decrease with the increase in sparsity, and γ is significantly greater than 1 while λ is close to 1; (b) In the range of sparsity from 0.1 to 0.36, σ decreases with the increase in sparsity but is always significantly greater than 1. HC, healthy control; PTSD, post-traumatic stress disorder; TEC, trauma-exposed control.

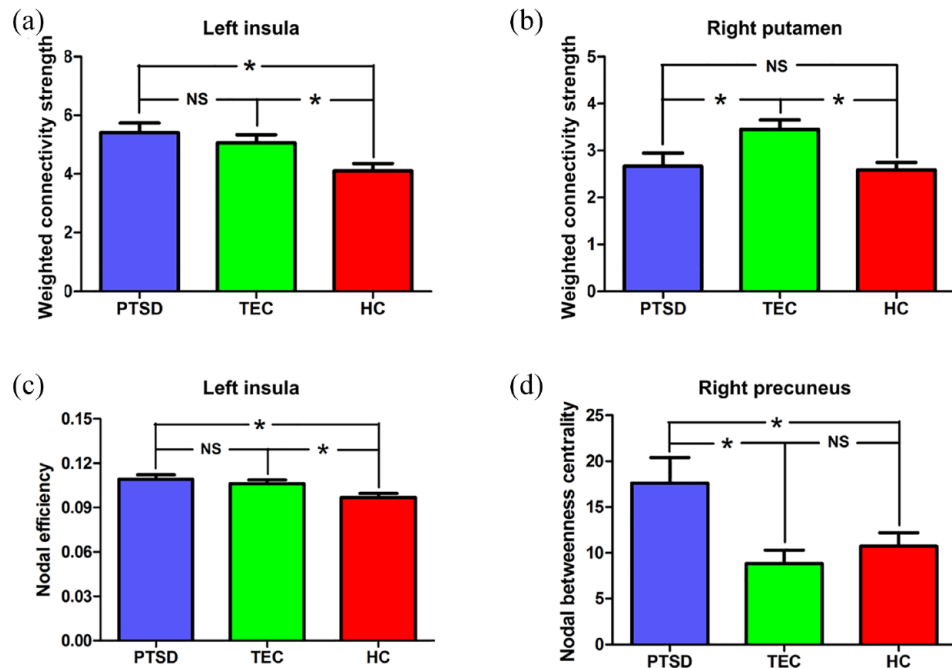


Figure 4. Results of the post hoc *t*-test for local parameters of the brain resting-state functional connectivity network. (a), (b), (c), and (d) show the group differences in the weighted connectivity strength of the left insula, the weighted connectivity strength of the right putamen, the node efficiency of the left insula, and the node mediation centrality of the right precuneus, respectively. HC, healthy control; PTSD, post-traumatic stress disorder; TEC, trauma-exposed control.

Correlation analysis results

The correlation analysis revealed no significant association between resting-state functional connectivity and the regional topology properties with the total CAPS score in the PTSD patients. The PCL score was positively correlated with the resting-state functional connectivity between the right

dACC-right paracentral lobule ($p=0.001$) and left dACC-left PoCG ($p=0.005$) but was negatively correlated with the resting-state functional connectivity between the right hippocampus-left PoCG ($p<0.001$)/right PoCG ($p<0.001$) and degree in the right putamen ($p=0.039$) across all traumatized subjects (Figure 5).

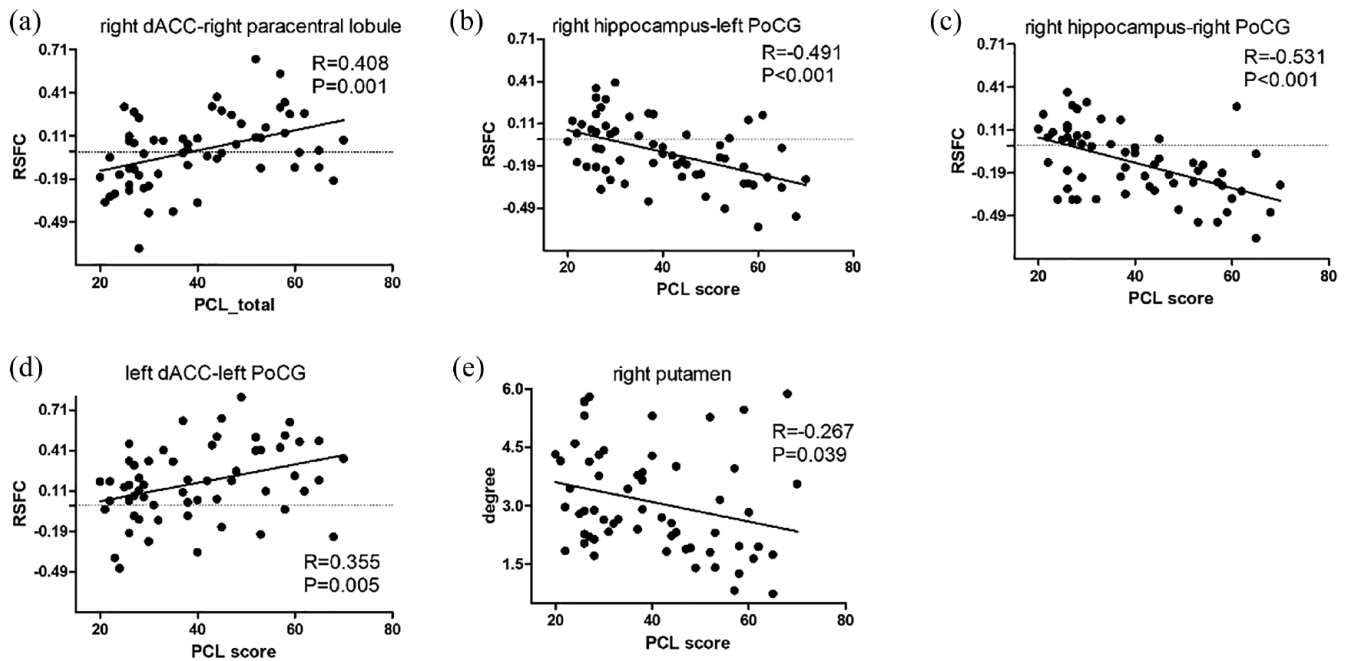


Figure 5. Results of correlation analyses between the functional index and PCL scores in all trauma-exposed subjects. The PCL score was positively correlated with the RSFC between the right dACC-right paracentral lobule (a) and left dACC-left PoCG (d) but was negatively correlated with the RSFC between the right hippocampus-left PoCG (b)/right PoCG (c) and degree in the right putamen (e) ($p < 0.05$, not corrected). dACC, dorsal anterior cingulate; PCL, PTSD checklist; PoCG, postcentral gyrus; RSFC, resting-state functional connectivity.

Discussion

This study analyzed and compared the global and local parameters of typhoon-experienced subjects' whole-brain resting-state functional connectivity network and HCs based on the AAL template. We found that the resting-state functional connectivity between the hippocampus and PoCG in the TECs was higher than in the PTSD patients and HCs. We also found that the PTSD patients showed enhanced resting-state functional connectivity between the dACC and the PoCG and paracentral lobule relative to the two control groups, implying that PTSD patients and TEC subjects have altered resting-state functional connectivity of brain region other than the DMN and SN. In addition, the whole-brain resting-state functional connectivity network of the three groups showed typical small-world properties, and the regional parameters of the insular lobe, putamen, and precuneus of the PTSD patients and TEC were abnormal.

The whole-brain resting-state functional connectivity analysis showed that the PTSD group had more robust dACC resting-state functional connectivity in the PoCG and paracentral lobule than the two control groups, suggesting that the

changes in dACC resting-state functional connectivity were relatively specific to PTSD. Unlike the ventral anterior cingulate cortex, primarily associated with emotional control, the dACC is considered related to cognitive function. It is a crucial brain area in the SN, playing an essential role in fear assessment, expression, and control of sympathetic nerve activity.³³ Although this study found that the dACC showed increased resting-state functional connectivity in PTSD patients, we could not determine whether this change in brain function was the cause or result of PTSD because we did not follow up with the subjects before or after PTSD onset. Interestingly, Shin *et al.* explored the brain function of twins using positron emission tomography and found that both veterans with PTSD and their twin brothers who did not experience military trauma had increased activity in the dACC under resting state conditions,³⁴ indicating that dACC dysfunction is a risk factor for PTSD rather than an acquired change.³⁵ In addition, the PoCG and paracentral lobule are parts of the sensorimotor network (SMN). Therefore, the results of this study may reflect high alertness, over-evaluation of threatening stimuli, and abnormal motor control in PTSD patients.³⁶

Lower negative resting-state functional connectivity between the hippocampus and the PoCG was found in the traumatized controls. The hippocampus is related to the encoding and recognition of declarative memory and plays a vital role in the discrimination of safe or dangerous environments and the extinction of conditioned fear.³⁷ Previous studies have also revealed that PTSD patients have hippocampal function abnormalities.^{38,39} The PoCG is related to the somatosensory experience. In this study, the negative resting-state functional connectivity of these two brain areas in the PTSD patients was relatively enhanced compared with the TECs, reflecting the weakening of the synergy between the two regions, which may have been associated with the aberrant integration and processing of environmental and somatosensory information in PTSD patients, ultimately leading to enhancement of the fear response.

Notably, although the resting-state functional connectivity between the hippocampus and the PoCG in the TEC group was enhanced compared with the PTSD and HC groups, the PTSD group did not show a statistically significant difference in resting-state functional connectivity compared with the HC group. Therefore, we believe that enhancing resting-state functional connectivity between the posterior central gyrus and temporal lobe structures such as the amygdala and hippocampus may be protective against the onset of PTSD.

In addition to the whole-brain resting-state functional connectivity analysis, we also explored the topological properties of the brain connectome. Similar to previous studies, the three groups all showed prominent small-world properties, and the local parameters of some brain regions in PTSD patients were abnormal.¹⁹⁻²¹ Notably, the TEC group showed a higher γ and σ of the brain resting-state functional connectivity network than the PTSD group and smaller values than the HC group. However, the differences among the three groups were not statistically significant. Previous studies have analyzed the brain function and topological properties of functional brain networks in PTSD related to earthquakes and found that the small-world properties of brain networks in PTSD patients are weaker than those in traumatized controls.^{20,21} The different results may be attributed to the different types of trauma. Importantly, we found that the small-world property of typhoon-related PTSD patients was

statistically weaker than in HCs when the effect of education level was not considered. Therefore, future studies must explore further whether educational level affects functional and structural small-world parameters.

Consistent with our results, resting-state brain function studies have found increased insular activity in individuals with PTSD or TEC compared with non-trauma-exposed individuals,^{40,41} suggesting that altered brain function in the insular cortex was caused by trauma. The insula is an essential part of the SN that monitors the body's internal state and predicts negative stimuli, in addition to playing a vital role in generating negative emotional processing and the fear response.^{42,43} Previous studies also found that compared with controls who had not experienced trauma, the resting-state functional connectivity of the insular lobe, amygdala, posterior cingulate cortex, and other brain regions in people with or without PTSD was significantly enhanced.⁴⁴⁻⁴⁸ Therefore, the increase of S_i and E_i in the insular lobe in the present study indicated that the resting-state functional connectivity of the SN, including the insular lobe, was increased, reflecting the persistent anxiety and high alertness of people who have experienced trauma in the resting state. However, unlike our findings, those of other studies revealed that the activity or resting-state functional connectivity of the insula in PTSD patients was significantly increased relative to TECs.^{12,20} The inconsistency may have been related to the higher PTSD symptom scores in the TEC group and the small sample size.

The putamen is part of the striatum and vital brain region of the SN, which plays a crucial role in motor control, reward prediction, and response.⁴⁹ Therefore, the relative decrease of S_i in the putamen of PTSD patients compared with traumatic controls may be related to abnormal reward processing, that is, the perception of pleasure is reduced and negative events such as pain are overestimated, which ultimately leads to the generation of negative emotions and cognition.⁴⁹ Previous resting-state studies have found that PTSD patients showed reduced striatal activity compared with TEC.^{50,51} Thus, our findings were consistent with those of previous studies, suggesting a relative decrease in regional brain activity or resting-state functional connectivity in the putamen in patients with PTSD. However, this study also found that the S_i of the putamen in the TEC group was higher than in the HC group,

whereas the PTSD and HC groups did not show a significant difference, suggesting that the higher Si of the putamen is a protective factor for the onset of PTSD. Partially consistent with this finding, Stark *et al.* found that striatal activity was significantly different between PTSD and TEC but not between PTSD patients and HC subjects.⁵²

In addition, the significantly higher BCi of the precuneus in the PTSD group suggested that the change in the BCi of the precuneus was specific to PTSD. The BCi measures the impact of a node on the exchange of information between other nodes in the network. As one of the core brain regions of the DMN, the precuneus is involved in autobiographical memory and self-reference processing and plays an essential role in integrating past and present information.^{44,53} The increase in the BCi in the precuneus of the PTSD patients in this study may have reflected the abnormal connection between memory and current environmental information, leading to the repeated reproduction of traumatic experience (memory). Besides, recent resting-state fMRI studies have revealed abnormal resting-state functional connectivity between the precuneus and amygdala, hippocampus, and other brain regions in PTSD patients.^{44,54,55} Similarly, one study also found that the local topological parameters of the precuneus were significantly enhanced in the earthquake-induced PTSD group compared with the TEC group.²⁰

The present study had several limitations. First, the sample size was relatively small. Second, this study was cross-sectional; thus, we could not definitively ascertain whether the alterations were specific to PTSD. Longitudinal studies should be performed in the future. Third, we only used an AAL template in this study. Different parcellation templates might show a variation in the nodal results. In addition, previous trauma exposure was not measured for all participants. Last, we only included typhoon-associated PTSD patients in the present study, so these results might not apply to other causes of PTSD.

In summary, this study results showed resting-state functional connectivity abnormalities in the SMN, SN, and DMN in PTSD patients. Both trauma and PTSD can lead to changes in the local parameters of the large-scale brain resting-state functional connectivity network. The enhancement in resting-state functional connectivity between the dACC and the PoCG, and the

paracentral lobule and the increase of BCi in the precuneus, are relatively specific to PTSD. Trauma can cause an increase in Si and Ei in the insular lobe, but PTSD may further aggravate the impairment of brain function. The enhancement of resting-state functional connectivity between the hippocampus and PoCG and the increase of Si in the putamen are protective factors for the onset of PTSD. Future studies should expand the sample size and follow up with the subjects to clarify the causal relationship between brain function changes and PTSD.

Declarations

Ethics approval and consent to participate

The need for approval for this study was waived by the ethics committee of our hospital and the Second Xiangya Hospital (Number 20140306). Written informed consents were obtained before the study began.

Consent for publication

Not applicable.

Author contributions

Hui Juan Chen: Conceptualization; Investigation; Methodology; Software; Supervision; Validation; Writing – original draft; Writing – review & editing.

Jun Ke: Conceptualization; Investigation; Methodology; Validation; Writing – original draft; Writing – review & editing.

Jie Qiu: Conceptualization; Methodology; Validation; Writing – review & editing.

Qiang Xu: Data curation; Formal analysis; Methodology; Project administration; Writing – review & editing.

Yuan Zhong: Data curation; Formal analysis; Methodology; Project administration; Writing – review & editing.

Guang Ming Lu: Data curation; Formal analysis; Methodology; Project administration; Writing – review & editing.

Yanglei Wu: Methodology; Writing – review & editing.

Rongfeng Qi: Conceptualization; Investigation; Methodology; Supervision; Validation; Writing – original draft; Writing – review & editing.

Feng Chen: Conceptualization; Investigation; Methodology; Supervision; Validation; Writing – original draft; Writing – review & editing.

Acknowledgements

The authors thank all the patients and volunteers for their participation.

Funding

The authors disclosed receipt of the following financial support for the research, authorship, and/or publication of this article: This work was supported by the National Natural Science Foundation of China (grant numbers 81971602; 82160327, 82271977; 8216070075, 81801684; 81871346, 81871344; 81701669), the Key Science and Technology Project of Hainan Province (ZDYF2021SHFZ239), the Hainan Academician Innovation Platform Fund, the Hainan Province Clinical Medical Center and the Chinese Key Grant (grant numbers BWS11J063, 10z026). This work was also supported by the Hainan Provincial Natural Science Foundation of China (grant number 818MS124), the Program of Hainan Association for Science and Technology Plans to Youth R & D Innovation (grant number QCXM201919), and the Nature Science Foundation of Jiangsu Province (grant number BK20170368).

Competing interests

The authors declared no potential conflicts of interest with respect to the research, authorship, and/or publication of this article.

Availability of data and materials

The datasets used during the current study are available from the corresponding author upon reasonable request.

ORCID iD

Feng Chen  <https://orcid.org/0000-0002-9129-7895>

Supplemental material

Supplemental material for this article is available online.

References

1. Svenaeus F. *Diagnosing mental disorders and saving the normal: Diagnostic and statistical manual of mental disorders*, 5th ed. Washington, DC. Medicine, Health Care, and Philosophy, American Psychiatric Publishing, 2013.
2. Nemeroff CB, Bremner JD, Foa EB, *et al.* Posttraumatic stress disorder: a state-of-the-science review. *J Psychiatr Res* 2006; 40: 1–21.
3. Michopoulos V, Norrholm SD and Jovanovic T. Diagnostic biomarkers for posttraumatic stress disorder: promising horizons from translational neuroscience research. *Biol Psychiatry* 2015; 78: 344–353.
4. Watts BV, Schnurr PP, Mayo L, *et al.* Meta-analysis of the efficacy of treatments for posttraumatic stress disorder. *J Clin Psychiatr* 2013; 74: e541–e550.
5. Menon V. Large-scale brain networks and psychopathology: a unifying triple network model. *Trends Cogn Sci* 2011; 15: 483–506.
6. Andrews-Hanna JR. The brain's default network and its adaptive role in internal mentation. *Neuroscientist* 2012; 18: 251–270.
7. Seeley WW, Menon V, Schatzberg AF, *et al.* Dissociable intrinsic connectivity networks for salience processing and executive control. *J Neurosci: Off J Soc Neurosci* 2007; 27: 2349–2356.
8. Lanius RA, Frewen PA, Tursich M, *et al.* Restoring large-scale brain networks in PTSD and related disorders: a proposal for neuroscientifically-informed treatment interventions. *Eur J Psychotraumatol* 2015; 6: 27313.
9. Shang J, Lui S, Meng Y, *et al.* Alterations in low-level perceptual networks related to clinical severity in PTSD after an earthquake: a resting-state fMRI study. *PLoS ONE* 2014; 9: e96834.
10. Kennis M, Rademaker AR, van Rooij SJ, *et al.* Resting state functional connectivity of the anterior cingulate cortex in veterans with and without post-traumatic stress disorder. *Hum Brain Mapp* 2015; 36: 99–109.
11. Yin Y, Jin C, Hu X, *et al.* Altered resting-state functional connectivity of thalamus in earthquake-induced posttraumatic stress disorder: a functional magnetic resonance imaging study. *Brain Research* 2011; 1411: 98–107.
12. Jin C, Qi R, Yin Y, *et al.* Abnormalities in whole-brain functional connectivity observed in treatment-naïve post-traumatic stress disorder patients following an earthquake. *Psychol Med* 2014; 44: 1927–1936.
13. Fornito A, Zalesky A and Breakspear M. The connectomics of brain disorders. *Nat Rev Neurosci* 2015; 16: 159–172.
14. Hosseini SM and Kesler SR. Comparing connectivity pattern and small-world organization between structural correlation and resting-state networks in healthy adults. *NeuroImage* 2013; 78: 402–414.

15. Sporns O and Zwi JD. The small world of the cerebral cortex. *Neuroinformatics* 2004; 2: 145–162.
16. Zhang J, Wang J, Wu Q, *et al.* Disrupted brain connectivity networks in drug-naive, first-episode major depressive disorder. *Biol Psychiatry* 2011; 70: 334–342.
17. Qin J, Wei M, Liu H, *et al.* Abnormal brain anatomical topological organization of the cognitive-emotional and the frontoparietal circuitry in major depressive disorder. *Magn Reson Med* 2014; 72: 1397–1407.
18. van den Heuvel MP, Mandl RC, Stam CJ, *et al.* Aberrant frontal and temporal complex network structure in schizophrenia: a graph theoretical analysis. *J Neurosci: Off J Soc Neurosci* 2010; 30: 15915–15926.
19. Long Z, Duan X, Xie B, *et al.* Altered brain structural connectivity in post-traumatic stress disorder: a diffusion tensor imaging tractography study. *J Affect Disord* 2013; 150: 798–806.
20. Lei D, Li K, Li L, *et al.* Disrupted functional brain connectome in patients with posttraumatic stress disorder. *Radiology* 2015; 276: 818–827.
21. Suo X, Lei D, Li K, *et al.* Disrupted brain network topology in pediatric posttraumatic stress disorder: a resting-state fMRI study. *Hum Brain Mapp* 2015; 36: 3677–3686.
22. Boccia M, D'Amico S, Bianchini F, *et al.* Different neural modifications underpin PTSD after different traumatic events: an fMRI meta-analytic study. *Brain Imaging Behav* 2016; 10: 226–237.
23. Weathers FLB, Herman D, Huska J, *et al.* *The PTSD checklist-civilian version (PCL-C)*. Boston, MA: National Center for PTSD, 1994.
24. Weng Y, Qi R, Chen F, *et al.* The temporal propagation of intrinsic brain activity associate with the occurrence of PTSD. *Front Psychiatry* 2018; 9: 218.
25. First MB, Spitzer RL, Gibbon M, *et al.* *Structured clinical interview for DSM-IV-TR axis I disorders, research version: patient edition (SCID-I/P) biometrics research*. New York: New York State Psychiatric Institute, 2002.
26. Weathers FW, Keane TM and Davidson JR. Clinician-administered PTSD scale: a review of the first ten years of research. *Depress Anxiety* 2001; 13: 132–156.
27. Zung WW. A rating instrument for anxiety disorders. *Psychosomatics* 1971; 12: 371–379.
28. Zung WW. A self-rating depression scale. *Arch Gen Psychiat* 1965; 12: 63–70.
29. Qi R, Luo Y, Zhang L, *et al.* FKBP5 haplotypes and PTSD modulate the resting-state brain activity in Han Chinese adults who lost their only child. *Transl Psychiat* 2020; 10: 91.
30. Fornito A, Yoon J, Zalesky A, *et al.* General and specific functional connectivity disturbances in first-episode schizophrenia during cognitive control performance. *Biol Psychiatry* 2011; 70: 64–72.
31. Jao T, Vértes PE, Alexander-Bloch AF, *et al.* Volitional eyes opening perturbs brain dynamics and functional connectivity regardless of light input. *NeuroImage* 2013; 69: 21–34.
32. Lynall ME, Bassett DS, Kerwin R, *et al.* Functional connectivity and brain networks in schizophrenia. *J Neurosci: Off J Soc Neurosci* 2010; 30: 9477–9487.
33. Etkin A, Egner T and Kalisch R. Emotional processing in anterior cingulate and medial prefrontal cortex. *Trends Cogn Sci* 2011; 15: 85–93.
34. Shin LM, Lasko NB, Macklin ML, *et al.* Resting metabolic activity in the cingulate cortex and vulnerability to posttraumatic stress disorder. *Arch Gen Psychiatry* 2009; 66: 1099–1107.
35. Admon R, Milad MR and Hendler T. A causal model of post-traumatic stress disorder: disentangling predisposed from acquired neural abnormalities. *Trends Cogn Sci* 2013; 17: 337–347.
36. Hayes JP, Hayes SM and Mikedis AM. Quantitative meta-analysis of neural activity in posttraumatic stress disorder. *Biol Mood Anxiety Dis* 2012; 2: 9.
37. Pitman RK, Rasmusson AM, Koenen KC, *et al.* Biological studies of post-traumatic stress disorder. *Nat Rev Neurosci* 2012; 13: 769–787.
38. Acheson DT, Gresack JE and Risbrough VB. Hippocampal dysfunction effects on context memory: possible etiology for posttraumatic stress disorder. *Neuropharmacology* 2012; 62: 674–685.
39. Zoladz PR and Diamond DM. Current status on behavioral and biological markers of PTSD: a search for clarity in a conflicting literature. *Neurosci Biobehav Rev* 2013; 37: 860–895.
40. Hughes KC and Shin LM. Functional neuroimaging studies of post-traumatic stress disorder. *Expert Rev Neurother* 2011; 11: 275–285.
41. Patel R, Spreng RN, Shin LM, *et al.* Neurocircuitry models of posttraumatic stress disorder and beyond: a meta-analysis of functional neuroimaging studies. *Neurosci Biobehav Rev* 2012; 36: 2130–2142.

42. Sripada RK, King AP, Garfinkel SN, *et al.* Altered resting-state amygdala functional connectivity in men with posttraumatic stress disorder. *J Psychiatry Neurosci* 2012; 37: 241–249.
43. Rabinak CA, Angstadt M, Welsh RC, *et al.* Altered amygdala resting-state functional connectivity in post-traumatic stress disorder. *Front Psychiatry* 2011; 2: 62.
44. Bluhm RL, Williamson PC, Osuch EA, *et al.* Alterations in default network connectivity in posttraumatic stress disorder related to early-life trauma. *J Psychiatry Neurosci* 2009; 34: 187–194.
45. van Wingen GA, Geuze E, Vermetten E, *et al.* Perceived threat predicts the neural sequelae of combat stress. *Mol Psychiatry* 2011; 16: 664–671.
46. Thome J, Frewen P, Daniels JK, *et al.* Altered connectivity within the salience network during direct eye gaze in PTSD. *Borderline Personal Disord Emot Dysregul* 2014; 1: 17.
47. Osuch EA, Willis MW, Bluhm R, *et al.* Neurophysiological responses to traumatic reminders in the acute aftermath of serious motor vehicle collisions using [15O]-H₂O positron emission tomography. *Biol Psychiatry* 2008; 64: 327–335.
48. Thomason ME, Marusak HA, Tocco MA, *et al.* Altered amygdala connectivity in urban youth exposed to trauma. *Soc Cogn Affect Neurosci* 2015; 10: 1460–1468.
49. Robinson BL and Shergill SS. Imaging in posttraumatic stress disorder. *Curr Opin Psychiat* 2011; 24: 29–33.
50. Kim SY, Chung YK, Kim BS, *et al.* Resting cerebral glucose metabolism and perfusion patterns in women with posttraumatic stress disorder related to sexual assault. *Psychiat Res* 2012; 201: 214–217.
51. Ke J, Zhang L, Qi R, *et al.* Altered blood oxygen level-dependent signal variability in chronic post-traumatic stress disorder during symptom provocation. *Neuropsychiatr Dis Treat* 2015; 11: 1805–1815.
52. Stark EA, Parsons CE, Van Hartevelt TJ, *et al.* Post-traumatic stress influences the brain even in the absence of symptoms: a systematic, quantitative meta-analysis of neuroimaging studies. *Neurosci Biobehav Rev* 2015; 56: 207–221.
53. Sartory G, Cwik J, Knuppertz H, *et al.* In search of the trauma memory: a meta-analysis of functional neuroimaging studies of symptom provocation in posttraumatic stress disorder (PTSD). *PLoS ONE* 2013; 8: e58150.
54. Sripada RK, King AP, Welsh RC, *et al.* Neural dysregulation in posttraumatic stress disorder: evidence for disrupted equilibrium between salience and default mode brain networks. *Psychosom Med* 2012; 74: 904–911.
55. Chen AC and Etkin A. Hippocampal network connectivity and activation differentiates post-traumatic stress disorder from generalized anxiety disorder. *Neuropsychopharmacology* 2013; 38: 1889–1898.